

Engineering approach to assess residual stresses in welded components

Dirk Schroepfer¹  · Arne Kromm¹ · Thomas Kannengiesser¹

Received: 2 November 2015 / Accepted: 27 October 2016 / Published online: 1 December 2016
© International Institute of Welding 2016

Abstract Present trends to lightweight design lead to an expanding relevance of high-strength fine-grained structural steels especially in mobile crane constructions. With growing material strength, the challenge for welding fabrication increases, since high loading capacities and safety requirements have to be accomplished. The utilisation of the high strength potential often requires complex constructions associated with high restraint conditions while welding. Increased residual stresses may occur due to superimposing reaction and restraint stresses, which have to be quantified and evaluated to ensure the safety and integrity of high-strength steel constructions. Particularly, the scope of residual stresses has to be taken into account for different effects in the HAZ, notches, weld and base metal. Commonly, conservative assumptions of residual stresses lead to distinct underestimations of the load bearing capacity particularly for welded high-strength steel constructions. This study concludes results of recent works of the researchers regarding the complex interaction among heat control, material and restraint intensity on the residual stress state in welded components. These analyses are extended by further experiments. Based on the obtained major effects, an approach for a welding residual stress assessment regarding

component design according to prevailing standards for crane construction, an important application for high-strength steels, is presented.

Keywords (IIW Thesaurus) Residual stresses · MAG welding · Restraint · High-strength steels · Process parameters

Nomenclature

a	Crack length
A	Cross section of the plate
b	Width of the plate
d	Thickness of the plate
E	Heat input
f_i	Characteristic load
F_j	Load
F_y	Reaction force transverse to weld
$F_{y,end}$	Transverse reaction force after cooling to RT
h	Height
$h_{W,n}$	Height of the weld at layer n
$h_{W,root}$	Height of the root weld
K_I	Crack driving force
L	Length
L_W	Length of the weld
M_x	Reaction moment of x -axis
$M_{x,end}$	Reaction moment after cooling to RT
R	Specific strength/characteristic resistance
R_{Fy}	Restraint intensity transverse to the weld
R_{Fy1}	Local restraint intensity
R_{Fy2}	Structural restraint intensity
R_{Fy3}	Nominal restraint intensity
R'_σ	Stress ratio with superimposed reaction stress
S_k	Load action at section k
t	Time
t_W	Welding time

Recommended for publication by Commission X - Structural Performances of Welded Joints - Fracture Avoidance

✉ Dirk Schroepfer
dirk.schroepfer@bam.de

Arne Kromm
arne.kromm@bam.de

Thomas Kannengiesser
thomas.kannengiesser@bam.de

¹ BAM Federal Institute for Materials Research and Testing, Berlin, Germany

T	Temperature
T_{Ed}	Reference temperature
T_i	Interpass temperature
T_p	Preheating temperature
$T_{p/i}$	Working temperature
v_H	Hoisting speed
W_x	Section modulus
x, y, z	Coordinates
α_W	Characteristic factor for limit weld stress
γ_m	Resistance coefficient
γ_n	Risk coefficient
γ_p	Partial safety factors
$\Delta t_{8/5}$	Cooling time of the weld from 800 to 500 °C
$\lambda(y)$	Local material properties
σ	Stress
σ_{Ed}	Reference stress level
σ_{hs}	Hot spot stress
σ_1	Resulting design stress at a specific location 1
σ_{11}	Stresses at specific location from load actions S_k
σ_{12}	Stresses at specific location from local effects
σ_m	Mean stress
σ_{max}	Maximum stress
σ_{min}	Minimum stress
σ_{Mx}	Bending stress
σ_{nlp}	Nonlinear stress peak
σ_{nom}	Nominal stress
σ_s	Load induced stress
σ_y	Reaction stress transverse to weld
$\sigma_{y,end}$	Transverse reaction stress after cooling to RT
$\sigma_{y,top}$	Total reaction stress on the top of the plate
σ_y^{rs}	Residual stress transverse to weld
$\sigma_{y,avg}^{rs}$	Average residual stress transverse to weld
$\sigma_{y,HAZ}^{rs}$	Residual stress level transverse to weld in HAZ
$\sigma_{y,max}^{rs}$	Maximum residual stress transverse to weld
$\sigma_{y,WM}^{rs}$	Residual stress level transverse to weld in WM
σ'_1	σ_1 including welding stresses
σ'_{11}	σ_{11} including welding stresses
σ'_{12}	σ_{12} including welding stresses
σ'_m	Mean stress with superimposed reaction stress
ϕ_i	Dynamic coefficients

1 Introduction

In a growing amount of industrial applications, high-strength fine-grained structural steels with yield strengths from 690 MPa are applied. The increasing trend towards light-weight design of today's steel constructions involves specific design solutions and economical aspects, like extensive reductions in weight and production costs, with increasing material strength [1]. Actual preferential applications are for instance mobile cranes or hydro power plants [2]. This leads to a wide variety of high-strength base and filler materials provided by

the steel producers [3]. However, a sustainable and economic application depends on the loading capacity and safety of welded components. To meet the advanced requirements of the mechanical properties in high-strength steel welds, the application of suitable filler materials and a heat control in an adequate working range (e.g. $\Delta t_{8/5}$ -cooling time) is necessary and sufficient hydrogen effusion and crack resistance have to be provided [4]. In this context, the avoidance of complex residual stress states is a considerable factor to increase the cracking resistance.

In particular, the components' safety and service life largely depend on the residual stress state of the welds. In component or repair welds, rigid restraint conditions are able to produce high tensile stresses due to welding [5, 6]. This is a consequence of the superposition of high reaction stresses due to supporting effects and occurring restraint stresses due to the inhomogeneous changes in the weld volume; see Fig. 1 [6]. High tensile residual stresses are known to compromise the integrity of welded components by a higher cold cracking risk and shorter lifetime to fracture [7]. Nevertheless, compressive residual stresses are oppositely able to compensate this. It is, therefore, important to avoid high tensile welding stresses in the heat-affected zone (HAZ) as well, which may be particularly critical due to degraded mechanical properties (grain coarsening, softening, etc.). An avoidance of fractures due to overloading is mainly achieved by an appropriate design. Frequently, high tensile stresses are promoted by an application of improper heat control and filler material under high restraints regarding the construction [8, 9].

Recent analyses involved high-strength steel welding under restraint conditions and showed significant influences of these factors for global and local stresses due to welding [10, 12–14]. However, it is oftentimes impossible to take advantage of all benefits from high-strength steels using prevailing codes and standards, e.g. EC3 [15], concerning high-strength steel processing. This is due to an insufficient quantitative forecast of the magnitude and location of residual stresses, e.g. the across-the-board assumption of residual stresses to the amount of the yield strength. Hence, at the beginning of

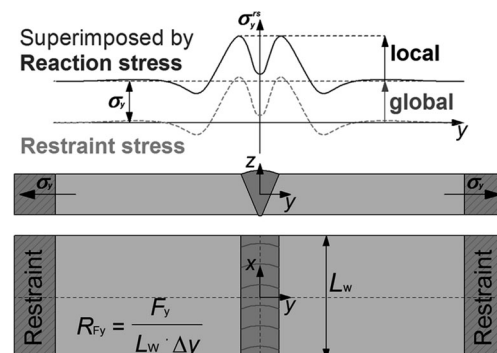


Fig. 1 Superposition of local and global welding stresses due to restraint intensity transverse to the weld [8, 10, 11]

this study, the theoretical analysis of real components regarding restraint is presented. Then, the investigations of the global and local welding stresses are described by means of component related weld tests. The restraint in the weld test was realised transverse to the weld. Hence, the distinguished evaluations, subsequently, consider magnitude and location of transverse welding stresses on the top side of the welds. This is done according to the prominent regions in analogy to the approaches of welded component assessment. From that, statements regarding welding stress optimisation for high-strength steel crane components can be elaborated.

2 Component transfer

In order to estimate the magnitude of each mentioned effect, component-related butt joints were welded in special in-house developed testing facilities. To maintain the transferability of the weld test results to real components, the restraint intensity of a typical welding application in a mobile crane was analysed. The concept of the restraint intensity was established by Satoh et al. [11] for a quantification and comparison of restraint conditions of different weld constructions. The restraint intensity in weld transverse direction R_{Fy} is the component stiffness towards the weld seam based on the seam length L_W and can be estimated for simple butt joints [6]; see Fig. 1. The restraint intensity determined in the weld detail of the crawler crane superstructure is $R_{Fy} = 1.5 \text{ kN}/(\text{mm mm})$ [12].

More severe testing conditions are represented in the testing facilities. Since the restraint intensity is based on the weld seam length L_W , a shorter weld increases the intensity of restraint. The restraint intensity determination within the test setup in the testing facilities was realised by the discretisation of the rigidity of the facility (nominal), the specimen dimensions (structural) and the weld seam (local); see Fig. 2. Whereas the nominal stiffness is constant for the testing facility, the restraint intensity can be varied significantly by means of the specimen dimensions (e.g. weld seam length and plate thickness) and the rigidity of the testing facility. In this study, the restraint intensity was varied from $R_{Fy} = 2$ to $4 \text{ kN}/(\text{mm mm})$.

3 Component weld tests

Subsequently, in the component tests, V-groove butt joints were automated multilayer MAG-welded at two different testing facilities for two plate thickness classes of $h = 8$ and 20 mm with the 0.5-MN- and the 2-MN-testing facilities respectively [12]. This allowed a simultaneous restraint while

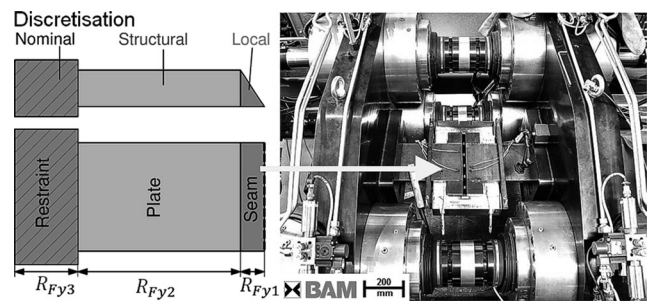


Fig. 2 Analytical determination of the restraint intensity [6] of the 2-MN-testing facility with a clamped specimen

welding and cooling as well as an in situ observation of the occurring reaction forces. High-strength quenched and tempered fine-grained structural steels S960QL and S690QL, according to EN 10025-6 [16], were analysed with similar high-strength solid filler wires, according to EN ISO 16834-A [17]. The chemical composition and mechanical properties of the test materials as well as the welding parameters are given in [12], which also provides the variation of interpass temperature, heat input, steel grade and restraint intensity altered by means of design of experiments (DoE). The restraint stresses in the weld seam were analysed using mobile X-ray diffraction and the $\sin^2\Psi$ -method on the top surface of the plates with applied restraint and after relaxation; see Fig. 3.

The welding process conditions were monitored in all weld tests. Therefore, the heat input was determined by the measurement of the actual values of welding current, voltage and speed. The heat control was observed by means of temperature measurements with type-K-thermocouples (preheat and interpass temperature) and with a two colour pyrometer directly on the weld seam (measuring range 350 to $1300 \text{ }^\circ\text{C}$). Thus, production-relevant process conditions (e.g. $\Delta t_{8/5}$ -cooling times) were maintained to provide the required micro structure and weld properties; see Fig. 4.

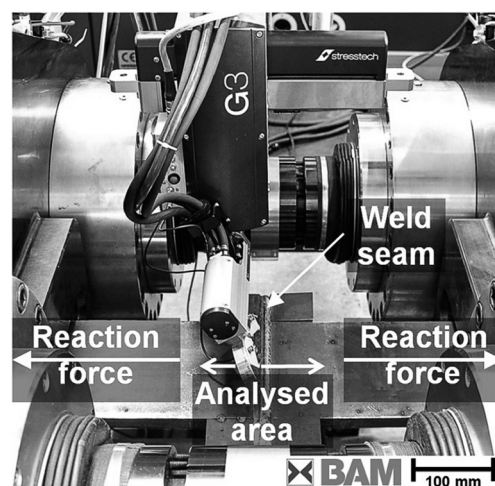
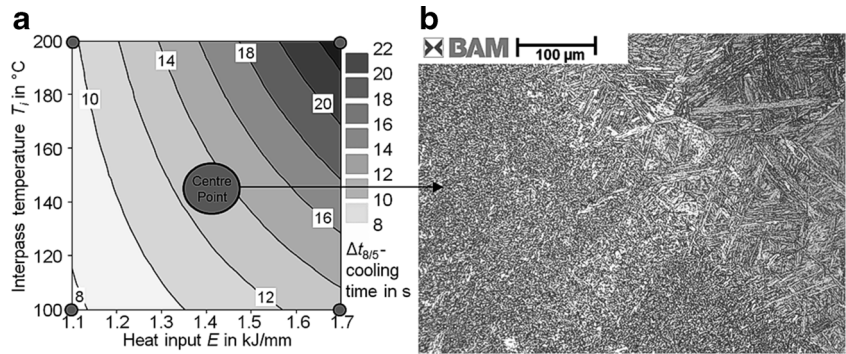


Fig. 3 Residual stress analysis of clamped specimens

Fig. 4 Heat control conditions for S690QL: **a** contour plot of the determined $\Delta t_{8/5}$ -cooling times vs. heat input and interpass temperature and **b** microstructure of weld and HAZ



4 Weld stress analyses

The residual stress state of a welded component is subjected to the complex interaction of its design, the welding process conditions and the applied materials; see Fig. 5. This work will review the results considering design and process conditions [8] and the analysis taking into account the applied materials and the welding process [12]. Those analyses of the previous works are extended by further experiments to satisfy a complete effect analyses according to Fig. 5.

4.1 Effect of design and process conditions

In [8], the reaction force $F_y(t)$ and temperature $T(t)$ were monitored in high-strength steel welds by using the 0.5-MN-testing facility. The effects of the process condition and the design were analysed by the variation of heat control and restraint intensity.

• *Global reaction stresses*

Following the evolution of the reaction force in Fig. 6a, while preheating of the tack welded specimen, a compressive reaction force persists. During root welding, a force buildup is obvious due to the shrinkage of the already solidified inserted weld metal, which generates transversal shrinking forces. While the root weld is cooling down to interpass temperature, the reaction force increases to a first maximum of $F_y = 58$ kN

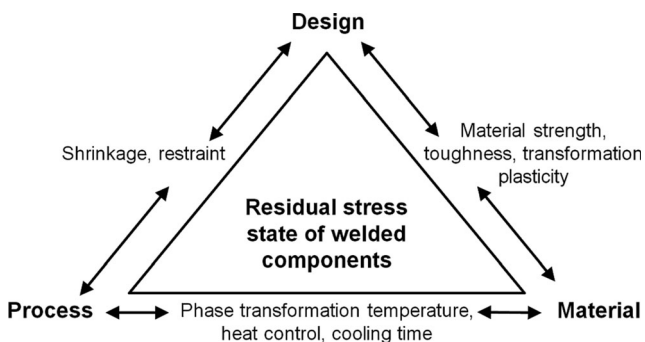


Fig. 5 Complex interaction of influences on the residual stress state in a welded component according to Karlsson [18]

at $T_i = 50$ °C. A force reduction is initiated by welding of the next layer due to local heat input combined with a transient volume expansion of the weld area and, hence, a stress relief. Again, cooling to T_i leads to a reaction force increase. This force evolution with an increase of the force amplitude was observed for every weld sequence. After the completion of the weld and subsequent cooling to ambient temperature, a maximum reaction force of $F_{y,end} = 90$ kN is reached. In Fig. 6b reaction forces $F_y(t)$ for weld tests using the 0.5-MN-testing facility with different interpass temperatures of $T_i = 50$ °C and

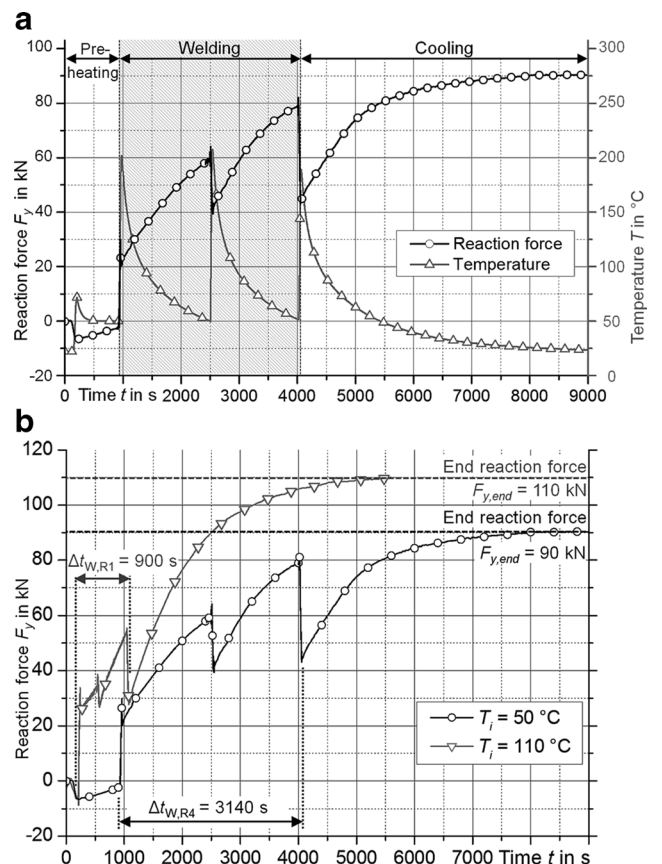
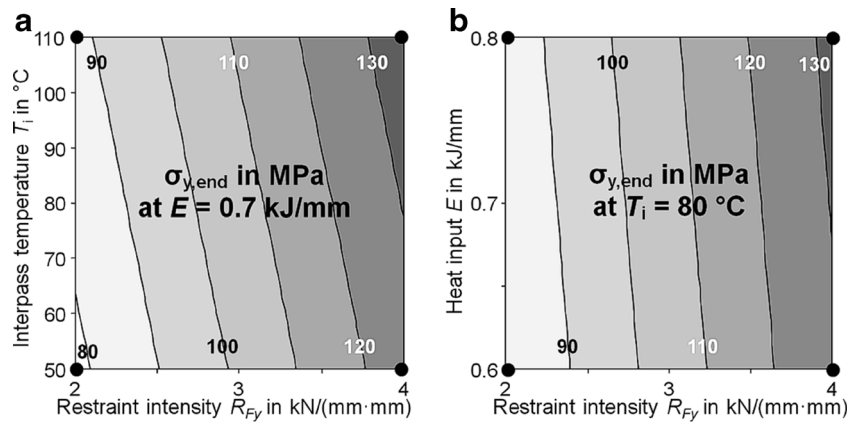


Fig. 6 Weld tests under defined restraint $R_{F_y} = 2$ kN/(mm mm) in the 0.5-MN-testing facility (S960QL, heat input $E = 0.6$ kJ/mm, three runs, preheat temperature $T_p = 50$ °C). **a** Reaction force $F_y(t)$ and temperature $T(t)$ for interpass temperature $T_i = 50$ °C. **b** Comparison of $F_y(t)$ for different interpass temperatures $T_i = 50$ °C and $T_i = 110$ °C

Fig. 7 Transverse reaction stress after cooling to ambient temperature $\sigma_{y,end}$ of S960QL (0.5-MN-testing facility): **a** vs. interpass temperature T_i and restraint intensity R_{Fy} (heat input $E = 0.7$ kJ/mm) and **b** vs. heat input E and restraint intensity R_{Fy} (interpass temperature $T_i = 80$ °C)



$T_i = 110$ °C are shown. The two $F_y(t)$ graphs exhibit the same tendency. Though, a high interpass temperature ($T_i = 110$ °C) leads to a reduction of total welding time by 70% and a lower level of the force amplitudes due to shorter cooling cycles. A higher heat level thereby remains between each weld run and causes decreased transverse shrinking forces and a reduced reaction force after the last weld run. However, this leads to a remarkable increase of the reaction force of $F_{y,end} = 110$ kN after subsequent cooling to ambient temperature.

The resulting end reaction stresses $\sigma_{y,end}$ were calculated from each $F_{y,end}$ based on plate cross section and statistically evaluated for the experimental design. These results are shown in Fig. 7 by contour plots vs. temperature and heat input. Varying the heat control between $T_i = 50$ and 110 °C, $E = 0.6$ to 0.8 kJ/mm and the restraint intensity between $R_{Fy} = 2$ and 4 kN/(mm mm) by means of DoE resulted in a major effect of the restraint intensity. A lower shrinkage restraint decreases the reactions stresses. Also, a reduced interpass temperature leads to lower reaction stresses (Fig. 7a). The effect of heat input is relatively small and not statistically significant (Fig. 7b) in the analysed parameter range.

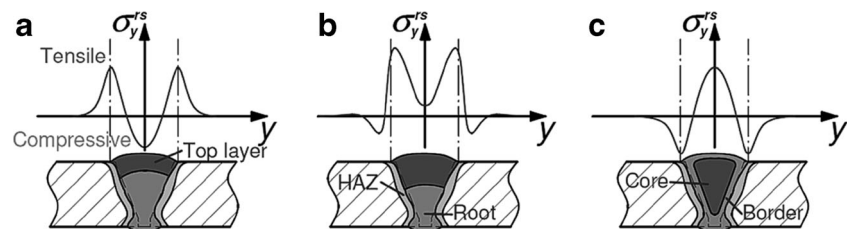
• *Local restraint stresses*

Local restraint stresses in the weld are due to the process conditions and material behaviour. They are a result of the superposition of three single components due to inhomogeneous

temperature distributions in weld and HAZ, i.e. shrinkage stresses, quenching stresses and transformation stresses [19, 20]. Whereas shrinkage stresses are always present in welds, quenching and transformation stresses are process and material specific. Transformation stresses are caused by a restrained volume expansion during the transformation from austenite to ferrite, bainite or martensite. All areas with undergoing austenitisation are affected involving weld and HAZ. Temperature gradients between the weld surface and the core areas may cause additional quenching stresses. Note that these three components are superimposed. Figure 8 shows typical transverse residual stress profiles across the weld according to common concepts [19]. These characteristic residual stress distributions are a consequence of the principal effect. The “M”-form (a) and the “W”-form (c) are idealised cases. A thin cap bead results in a homogeneous cooling and dominating compressive stress at the weld centre line due to phase transformation (a). In a bulky molten volume, an inhomogeneous transformation of core and border areas is caused. The delayed transformation of the core leads to characteristic tensile stress elevation at the surface of the weld centre (c). Typical stress profiles of actual welds are in-between of both cases. In case of Fig. 8b, additional quenching stresses lead to a stress dip in the weld centre and stress maxima next to the weld centre near the fusion line.

Primarily, residual stress measurements were performed at free shrinking specimens, welded with varied heat control parameters. Higher heat input and interpass temperature values lead to larger heated volumes while welding. As a result, a higher inhomogeneous shrinkage restraint occurs in

Fig. 8 Typical transverse residual stress distributions according to Nitschke-Pagel and Wohlfahrt [19]



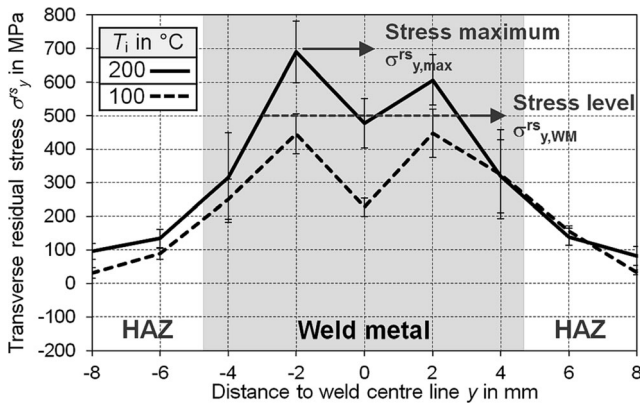


Fig. 9 Comparison of transverse residual stresses $\sigma_y(y)$ for two different interpass temperatures T_i (S960QL, 0.5-MN-testing facility, after relaxation, two runs, $T_p = 50\text{ }^\circ\text{C}$, $E = 0.8\text{ kJ/mm}$) [8]

combination with increasing tensile residual stresses [20]. Figure 9 shows the residual stress distributions for two welds, where a different interpass temperature was applied. The residual stress maxima and the level of the weld at high interpass temperature are significantly increased compared to weld at low interpass temperature.

- *Superposition of local and global stresses*

In Fig. 10a, transverse residual stress distributions of specimens welded under free shrinkage and welded under defined restraint ($R_{Fy} = 2\text{ kN/(mm mm)}$) are compared. Welding under additional restraint conditions causes an increase of the residual stress profile due to the occurring reaction stresses. Additional weld tests under a higher restraint intensity ($R_{Fy} = 4\text{ kN/(mm mm)}$) allowed a statistical evaluation of the effects of heat control and restraint condition on the transverse residual stress level. These average tensile residual stresses in the weld metal were calculated by Eq. 1 ($y_1 = -6\text{ mm}$, $y_2 = +6\text{ mm}$) [12].

$$\sigma_{y,avg}^{rs}(y_1 \dots y_2) = \left(\frac{1}{(y_2 - y_1)} \right) \int_{y_1}^{y_2} \sigma_y^{rs}(y) dy \quad (1)$$

Fig. 10 a Transverse residual stress distributions $\sigma_y(y)$ of 8 mm thick S960QL specimens welded under free shrinkage and under restraint ($R_{Fy} = 2\text{ kN/(mm mm)}$) and **b** average transverse residual stress $\sigma_{y,WM}^{rs}$ vs. interpass temperature and restraint intensity at heat input $E = 0.6\text{ kJ/mm}$

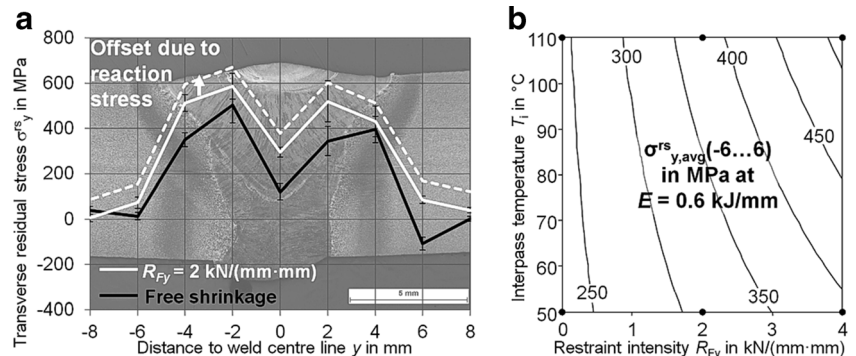


Fig. 10b shows the contour plot of the determined stress levels as a function of interpass temperature and restraint intensity at heat input $E = 0.6\text{ kJ/mm}$. Obviously, not only the increased restraint intensities cause higher stress levels but also a growing influence of the interpass temperature.

4.2 Effect of material and process conditions

In [12], effects of process conditions and material were primarily investigated. Therefore, the occurring welding stresses in weld tests using the 0.5-MN- and the 2-MN-testing facilities were analysed for two different steel grades with varied heat control parameters. These investigations were extended by additional component analyses in the present work to conclude a complete effect analysis.

- *Global reaction stresses*

Figure 11 shows the reaction stress buildup of two component tests of S690QL welded with different interpass temperatures. The reaction forces were measured via load cells directly at the test frame of the 2-MN-testing facility. The momentary reaction stress was calculated based on the actual weld height from a macrograph and the reaction force; see Eq. 2:

$$\sigma_y(t) = \frac{F_y(t)}{h_{W,n} \cdot b} \quad (2)$$

It is obvious that higher interpass temperatures lead to lower amplitudes of reaction stress in the component welds as well; see Fig. 6. Comparing both tests, a $60\text{ }^\circ\text{C}$ lower interpass temperature results in a 15% lower end reaction stress after cooling to ambient temperature. However, especially during the cooling of the root weld to a reduced interpass temperature, high stresses could be reached due to the small load bearing section. In this case, a reaction stress maximum of approx. 140 MPa is gained. Note that this value is even higher than the end reaction stress. In high-strength steel fabrication, this behaviour is taken into account by the application of more

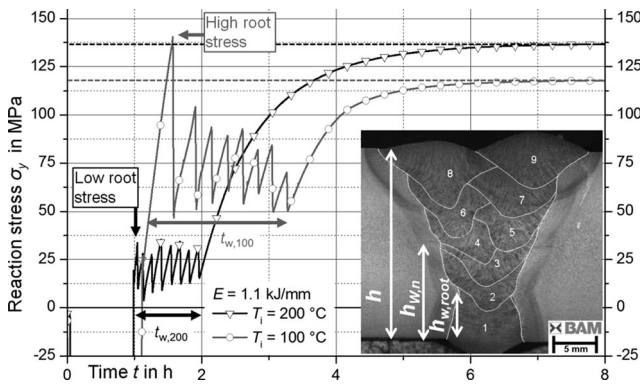


Fig. 11 Comparison of reaction stresses $\sigma_y(t)$ for two different interpass temperatures T_i (S690QL, 2-MN-testing facility, nine runs, $E = 1.1$ kJ/mm, $T_p = 120$ °C)

ductile filler metals for the root to avoid its cracking. Thus, for the component analyses of the S960QL with 20 mm plate thickness, a lower strength solid wire G 46 according to EN ISO 14341-A [21] was applied for the root weld.

Based on the results of [12], the variation of the factors was extended to a parameter matrix by means of DoE. The result of the statistic evaluation (variance analysis) of the end reaction stresses for the complete parameter matrix is shown in Fig. 12 for both materials, S690QL and S960QL. First, it should be noted that the effect of interpass temperature and heat input is significant in both steel grades, which agrees with earlier studies [13, 14]; see also Fig. 6. Though, comparing the contour plots of both materials, a remarkable increase of the end reaction stresses in the welds of the lower strength steel grade reveals for the whole parameter range. The reasons are a different transformation behaviour of the weld metal and HAZ heated above austenisation temperature and a different resulting microstructure, pointed out in [12] and also in [22] according to other recent works, e.g. [23].

- *Local restraint stresses*

Fig. 12 End reaction stresses $\sigma_{y,end}$ for component weld tests as a function of interpass temperatures and heat input, for base material **a** S690QL and **b** S960QL

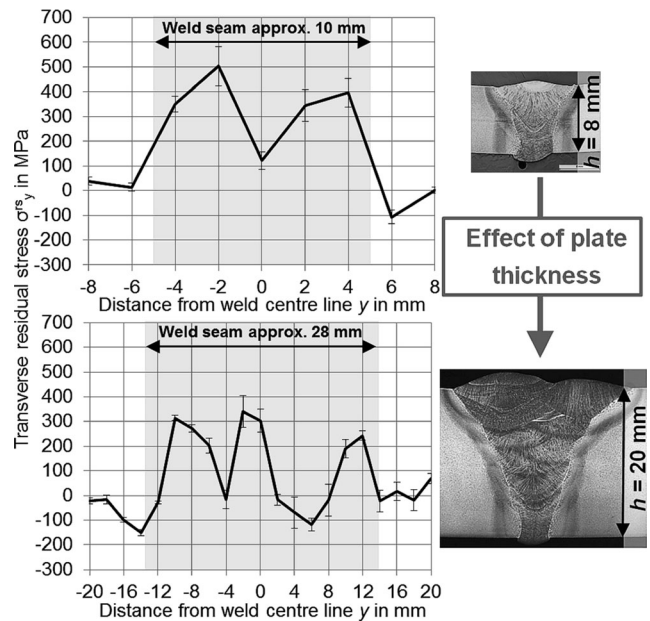
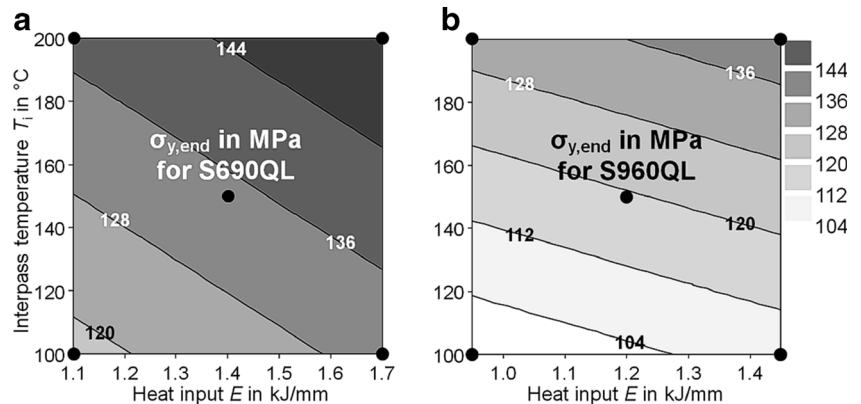


Fig. 13 Comparison of transverse residual stresses $\sigma_y^{rs}(y)$ for two different plate thicknesses $h = 8$ and 20 mm (S960QL, welded under free shrinkage)

Comparing the residual stress distributions across the welds of specimens in 8 and 20 mm thickness, a more complex stress profile is obvious in the latter; see Fig. 13. Multiple weld beads at the top of the weld and different conditions of heat conduction in the through-thickness direction in thicker plates lead to an extensive interaction of each effect due to phase transformation, annealing and quenching. Thus, a comparison and evaluation of surface-near residual stresses are more difficult in welds of thicker plates.

- *Superposition of local and global stresses*

In Fig. 14, two transverse residual stress distributions above the weld of S690QL specimens with different interpass

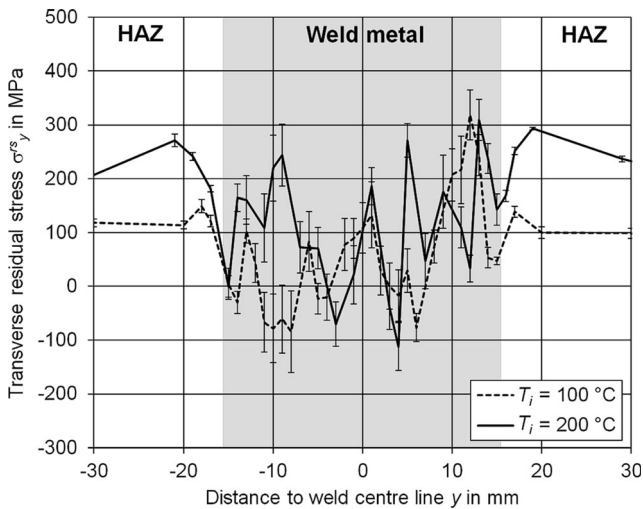


Fig. 14 Comparison of transverse residual stresses $\sigma_y^{rs}(y)$ for different interpass temperatures T_i (2-MN-testing facility, S690QL, six runs, $E = 1.7$ kJ/mm, $T_p = 120$ °C) [12]

temperatures are compared. From the stress distributions in the weld metal, no significant differences can be found considering local residual stress maxima and magnitudes. Statistic evaluations of the residual stress maxima and levels of both analysed steel grades show a minor trend that higher interpass temperatures effect increased and broader stress profiles at high heat input [12].

However, the residual stress magnitude of the HAZ exhibits a disproportionately high increase in the restrained test specimens due to high interpass temperatures. Equation 1 was used to quantify the residual stress magnitude of certain weld areas according to [12]. For the quantification of the level of the transverse residual stresses in the HAZ, the distance range from the weld centre line of ± 15 to 30 mm was applied. The determined values were statistically evaluated by means of variance analysis of the parameter matrix of both steel grades. The results are shown in Fig. 15 by contour plots of the average transverse residual stresses of the HAZ $\sigma_y^{rs,HAZ}$ vs. heat input and interpass temperature.

Fig. 15 Average transverse residual stresses in the HAZ $\sigma_y^{rs,HAZ}$, centre of component specimens ($x = 0$ mm) vs. interpass temperature T_i and heat input E , for base material **a** S690QL and **b** S960QL

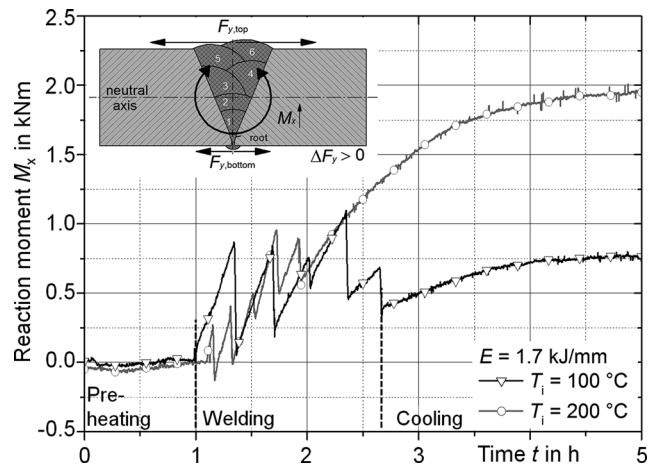
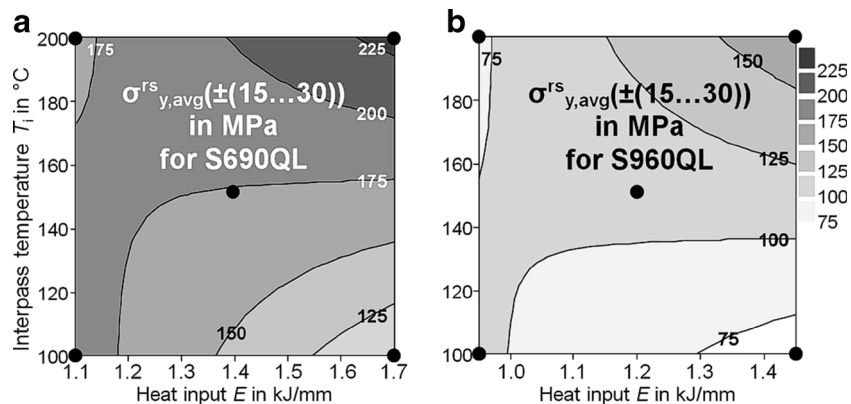


Fig. 16 Comparison of bending moments $M_x(t)$ for S690QL component weld tests with different interpass temperature at constant heat input $E = 1.7$ kJ/mm

It is obvious that the application of a high heat input and a low amount of weld beads respectively, leads to a significant effect of the interpass temperature. In both steel grades, the difference between the magnitudes of residual stresses in the HAZ is about 100 MPa, whereas almost no difference could be found for low heat input values. A possible cause for the higher welding stresses in the HAZ is an increased reaction stresses. These bending moments are a result of the completely restrained specimen, which also results in hindered angular distortion. The three-dimensional servo-hydraulically controlled system of the 2-MN-testing facility allows a multiaxial load analysis of the welded component [13]. Hence, the build-up of the resulting bending moments was measured and is shown for two weld tests with high heat input and different interpass temperatures in Fig. 16.

Both graphs of the bending moments $M_x(t)$ are qualitatively similar. It is obvious that already after the welding of the root, a lower reaction moment appears in the specimen if a higher interpass temperature was applied due to a shorter cooling phase. While the cooling of the first filler bead, the difference between both bending moments is approx.

Table 1 Resulting reaction stress on the top of weld of 2-MN-test specimens of S690QL, $E = 1.7$ kJ/mm

T_i in °C	$\sigma_{y,end}$ in MPa	M_x/W_x in MPa	$\sigma_{y,top}$ in MPa
100	129	56	185
200	152	146	298

Section modulus $W_x = b \cdot h^2 \cdot \frac{1}{6}$, $b = 200$ mm, $h = 20$ mm

$\Delta M_x = 0.5$ kNm. However, welding of the second layer leads to complete reduction of the reaction moment due to the heat input at the top of the root weld. Analogous to the reaction force buildup, this behaviour repeats for each weld sequence. The ratio of bending moment increase to decrease in average for each layer is greater than one. After welding of the top layer in the weld of elevated interpass temperature, the bending moment is approx. $\Delta M_x = 0.2$ kNm higher. Cooling to ambient temperature leads to an end reaction moment of $M_{x,end} = 1.95$ kNm at high interpass temperature, compared to $M_{x,end} = 0.75$ kNm at low interpass temperature. The bending moment is a result of the difference between the reaction force of the top and the bottom of the weld. As a consequence, the reaction stress at the top of the weld is higher for a positive bending moment. The resulting total reaction stress of the weld top site can be calculated by Eq. 3:

$$\sigma_{y,top} = \frac{F_y}{A} + \frac{M_x}{W_x} \quad (3)$$

In Table 1, the resulting local reaction stresses considering hindered angular distortion $\sigma_{y,top}$ are shown for both component welds of S690QL; see Fig. 16. The difference of the reaction stress on top of the weld between both specimens is approx. $\Delta \sigma_{y,top} = 113$ MPa. This value is in good agreement with the differences measured using X-ray diffraction analyses in the HAZ; see Fig. 15a. Similar effects were found for the higher strength steel S960QL shown in Fig. 15b. Remarkably, the resulting reaction stresses and stress level in the region of the HAZ are significantly decreased compared to the S690QL steel grade [12] due to a different behaviour considering phase transformation.

4.3 Conclusion of the analyses

From the results, it can be stated that the common concepts for residual stresses in welds are appropriate [20, 24]. However, an improved assessment of the residual stresses especially in welded components of high-strength steel is necessary. Furthermore, the effects of design, material and process on the residual stresses are subjected to a particular weld region; see Fig. 17. The location of the highest residual stresses and the combination of influence factors leading to critical values have to be indicated. Thus, a simultaneous consideration of the critical regions of the weld seam and the load type is

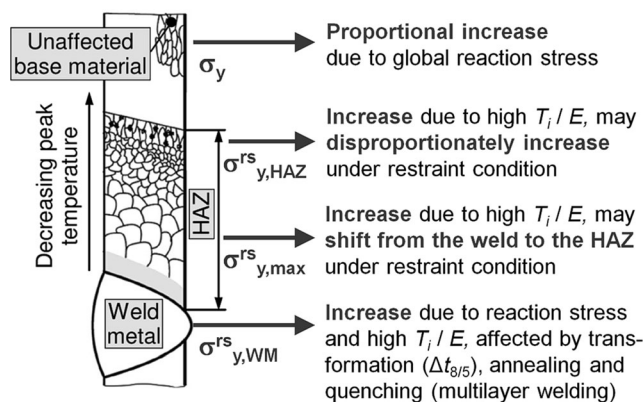


Fig. 17 Schematic of different weld regions, major influences on the residual stresses in a component weld

necessary. Particularly, the scope of residual stresses has to be taken into account for the different effects in the HAZ, weld metal, base metal and notches (e.g. fusion line). From the analyses, the different effects for each zone in a welded component can be concluded:

- *Base material*

The effect on the base material of welded components is due to the global reaction stresses. The reaction stresses increase if high preheat, interpass temperatures and high heat inputs are applied. Increasing restraint intensities augment the influence of heat control. The use of higher strength steel grades in filler beads may lead to lower reaction stresses due to an increased compensation of tensile stresses during phase transformation.

- *Heat-affected zone*

The transition from the weld metal to HAZ is characterised by high residual stress gradients. Increasing transverse residual stresses were observed coming from the fusion line. After a maximum, the residual stresses are declining towards the base material stress level, which is primarily affected by global reaction stresses. Generally, the transverse residual stress level was observed to be lower in the HAZ compared to the weld metal. However, in welded components, a superposition of the global reaction stresses and increasing bending moments may occur if the lateral and angular distortion of the weld is restrained. Then, major effects are given by a high heat input and high interpass temperature, especially in the case of the lower strength steel grade S690QL. One consequence is a disproportionately high increase of the residual stresses in the HAZ, which was also shown for large component tests by [10].

- *Residual stress maxima*

In prevailing standards and guidelines, the assumption of maximum residual stresses on the amount of yield strength is common. As shown, in high-strength steels, the highest observed residual stresses on the surface of the top layer were not higher than 50 to 70% for typical restraint intensities measured with X-ray diffraction. The magnitude of the residual stress maxima is rather affected by the factors discussed above. Transverse residual stress profiles in steels with an undergoing phase transformation are characterised by stress maxima in the weld metal somewhat next to the weld centre line. The weld centre line typically shows a stress dip due to quenching and transformation stresses. If more than one cap bead is necessary, these maxima occur next to the centre line of the last cap bead. Cap beads welded before show rather lower secondary maxima due to annealing effects. High interpass temperatures and high heat inputs lead to increasing stress maxima magnitudes. Under restraint, the involved superposition of the reaction stresses additionally intensifies the effect of heat control. In thicker plates, where more than one cap bead is necessary, a complex interaction of quenching, transformation and annealing due to bulky molten volumes occurs. Therefore, the residual stress maxima on the weld metal surface are difficult to compare. Note that leaving the parameter range by means of $\Delta t_{8/5}$ -cooling time may not only decrease the mechanical properties of the weld but also generate higher stress maxima. Since the stress maxima are located in the weld metal, usually free from notches, it cannot be spoken of critical stresses due to plastification effects during loading. However, as discussed above, a disproportional high increase of the residual stresses in the HAZ due to restraint conditions may lead to a shift of the transverse residual stress maxima towards the fusion line and HAZ. High residual stress magnitudes in the HAZ are especially detrimental due to crack critical microstructures (e.g. grain coarsening, softening).

- *Fusion line*

At the transition from the weld metal to HAZ, an avoidance of high residual stresses is important as well. Since the role of notches dominates mechanical behaviour of welded high-strength steels, especially under cyclic load [25], high tensile residual stresses may additionally cause disadvantageous effects considering the component lifetime.

- *Weld metal*

As discussed above, transverse residual stress levels in the weld metal increase with high heat input and interpass temperature. Restraint conditions of welded components, causing reaction stress superposition, increase the effect of heat control. As for the residual stress maxima, the quantification of

the effect is more complex for thicker plates due to multilayer welding.

5 Weld stress assessment

Finally, Fig. 18 schematically presents a concept for an evaluation of the analysed residual stresses. The derived statements for the effects on the residual stress state are transferred to the approaches of welded component assessment. Consequently, global reaction stresses affecting components are nominal stresses. A superposition with load-induced stresses should be evaluated according to the nominal stress approach [26]. With the analysis of average tensile residual stresses, residual stress levels for different scopes could be derived. These stress levels should be evaluated according to the structural stress approach [27].

In some cases, a consideration of tensile residual stress maxima is necessary, especially when they are located in crack critical regions, for instance notches or detrimental microstructures of the HAZ. An unfavourable location of the stress maxima may necessitate a highly conservative component design. From this point of view, it is reasonable to take high residual stress gradients into account, since they commonly appear in transition regions of welds. Therefore, another possibility is a component assessment regarding the notch stress approach [28]. The inclusion of residual stresses in the strength assessment should consider quasi-static and dynamic loads. Hence, diversified aspects regarding load, location and different types of welding stresses should be provided by coefficients (e.g. stress concentration factors or notch factors). With help of diversified welding stress analyses and evaluations, an advanced optimisation of residual stresses due to

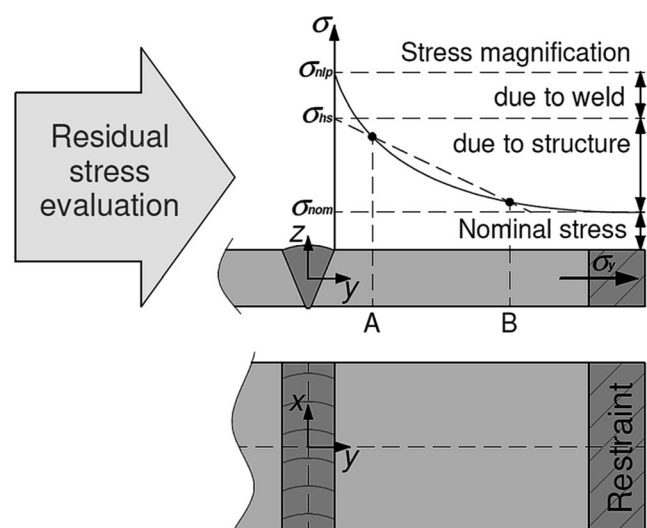
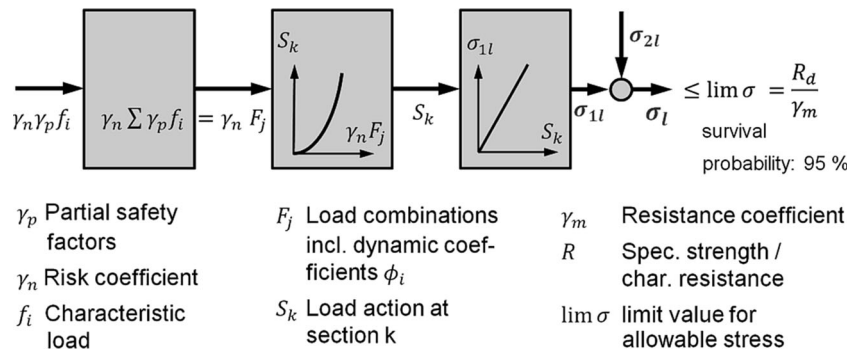


Fig. 18 Schematic evaluation of welding stresses by transferring the given statements to the approaches of welded component assessment according to Hobbacher [29]

Fig. 19 Flow chart for the proof of strength in crane component design using limit states method according to EN 13001 [30]



welding of high-strength steel components is achievable, in order to take advantage of the technical and economic benefits of those steel grades. The approach presented is based on the design codes for the crane construction EN 13001 [30] and mobile crane construction EN 13000 [30], since it is one of the most important applications of high-strength fine-grained structural steels.

5.1 Proof of strength in crane components

The design and assessment of components depends on which load condition dominates. In mobile crane fabrication, generally, a quasi-static load condition is assumed according to EN 13000 [31] and FEM 5.004 [32]. Occurring regular dynamic loads are then considered applying dynamic coefficients dependent on the load combination. If occasional loads from load combinations (e.g. environmental effects) occur frequently enough, then limit values for the design stress may be calculated according to the nominal stress approach applying characteristic fatigue strength values according to EN 13001 [30].

For the design of mobile crane structures [30–32], residual stresses in welded components are only taken into account if loads and stresses are transferred in transverse direction to the weld. Therefore, Fig. 19 shows a flow chart for the proof of strength of a critical location using the limit states method for the design of a load bearing crane component. Individual characteristic loads f_i extended with the dynamic coefficients ϕ_j and multiplied with partial safety factors γ_p are combined to load combinations F_j . Depending on safety restrictions, risk coefficients γ_n have to be multiplied to the combined loads. Based on that result, the determination of the load action S_k at the specific section k can be conducted. The stress σ_{1l} for a specific component is then calculated from the section specific load actions. Additional stresses due to local influences σ_{2l} (e.g. stress concentration and localised stress) may be subjoined for the determination of the design stress σ_l at a specific location l .

Instead of an over-the-board-assumption of residual stresses by safety factors, the realistic residual stress characteristics

and profiles should be taken into account. Therefore, residual stress magnitudes and locations have to be quantified. For a consideration and assessment of welding stresses in the component design according to [30–32], the following approaches are suggested:

5.2 Nominal stresses

As shown above in Figs. 7 and 13, the global reaction forces in a welded component transverse to the weld direction could be approximated by a function of the restraint intensity and the heat control parameters for a given material. A database would help derive good estimations, which could, e.g. be connected to numerical determinations of the restraint intensity. Since the reaction stresses in a weld are assumed to be constant across the thickness, a consideration as nominal stresses is suggested; see Fig. 20. In case of quasi-static load condition, the design stress σ'_l can be calculated by a superposition of the load-induced stress σ_s and the reaction forces; see Fig. 21a and Eq. 4.

$$\sigma'_l = \sigma_s + \frac{F_y(E, T_{p/i}, R_{Fy})}{A} = \sigma_s + \sigma_y(E, T_{p/i}, R_{Fy}) \quad (4)$$

Thus, the inclusion in beam modelling for assessment calculation, e.g. for FEA, is practicable.

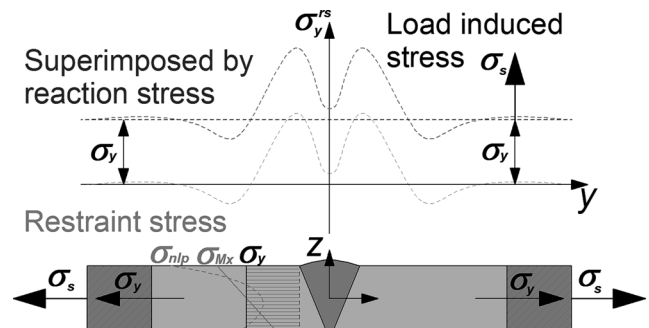
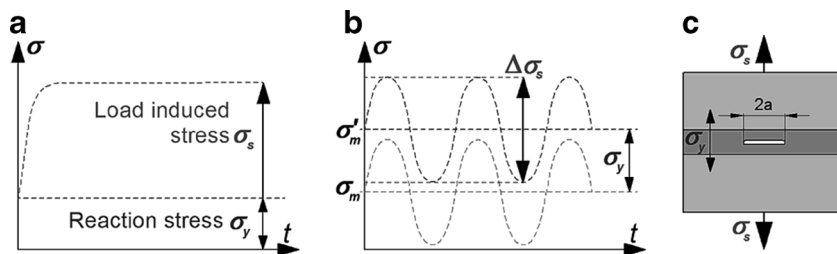


Fig. 20 Superposition of welding and load induced stress according to nominal stress approach

Fig. 21 Superposition of welding and load induced stress according to nominal stress approach for different load conditions, **a** quasi-static load, **b** cyclic load and **c** crack in weld metal



If reaction stresses are superimposed by cyclic loading, as shown in Fig. 21b, not the stress range, but the stress ratio (Eq. 5.1) and, therefore, the mean stress (Eq. 5.2) are affected:

$$R'_\sigma = \frac{\sigma_{\max} + \sigma_y}{\sigma_{\min} + \sigma_y} \tag{5.1}$$

$$\sigma'_m = \sigma_{\max} - \sigma_{\min} + \sigma_y \tag{5.2}$$

Thus, reaction stresses influence the lifetime of a welded component. The lifetime is reduced due to the mean stress effect. The sensitivity of specific materials in the face of increased mean stresses can be derived from Haigh-diagrams [33], which are also given in [30]. In case of cracks in the weld, as shown in Fig. 21c, welding stresses have to be considered in fracture mechanics. Therein, reaction stresses directly superimpose load-induced stresses and affect the crack driving force K_I as primary stresses [34]. Corresponding to quasi-static and cyclic load conditions, the knowledge about global welding stresses is helpful for the determination of the critical load and the residual lifetime respectively. In the nominal stress approach, coefficients help to take local influences, such as notches, surface conditions and material, into account. However, local influences are not considered directly, which oftentimes results in conservative designs. For assessments with improved precision, local approaches are necessary [27, 28].

5.3 Local structural stresses

In analogy to the structural stress approaches, local residual stresses can be considered, since whole regions are affected. If the strength in a critical spot (referred as hot spot) should be proven, the local welding stresses are of interest. In the case of increased residual stress level in the surface near regions of the HAZ, significant adverse effects on the design stress are expectable; see Figs. 14 and 15. For the strength assessment of a welded component, a consideration as additional stresses due to local influences σ_{21} is necessary; see Fig. 19.

As shown in Fig. 22, the local effect of the increased residual stress level may be due to high reaction moments as a result of the restrained angular distortion. Then, welding stresses are observable due to a locally increased residual

stress level $\sigma^{rs}_{y,avg}(HAZ)$ from X-ray diffraction analyses as well as bending moments σ_{Mx} from global reaction force measurements. Because of the application of average stresses in the HAZ, the nonlinear stress peak σ_{nlp} remains disregarded. Moreover, the result is an additional stress increase due to local influences σ'_{21} at the specific section. This has to be considered in the strength assessment of a high-strength steel weld applying Eqs. 6.1 to 6.4:

$$\sigma'_1 = \sigma'_{11} + \sigma'_{21} \tag{6.1}$$

$$\sigma'_{11} = \sigma_s + \sigma_y \left(E, T_{p/i}, R_{Fy} \right) \tag{6.2}$$

$$\sigma'_{21} = \sigma_{Mx} = \frac{M_x(E, T_{p/i}, R_{Fy})}{W_x} \tag{6.3}$$

$$\sigma'_{HAZ} = \sigma_s + \sigma^{rs}_{y,HAZ}(E, T_{p/i}, R_{Fy}) \tag{6.4}$$

The local stress increase is a consequence of the global forces and moments. Hence, an effect due to the mean stress effect on the lifetime is given regarding cyclic loading. The residual stress levels in the weld metal in same direction as the load direction may be taken also into account. Note that if no notch or critical microstructure persists at the weld metal itself, effects of stress concentration and local reduced mechanical properties can be excluded. Under the assumption of sufficient toughness of the material, residual stress levels in

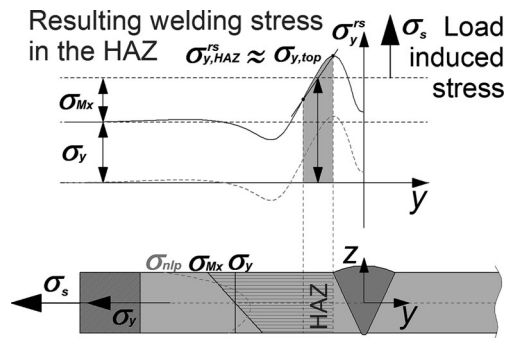


Fig. 22 Superposition of welding and load induced stress according to structural stress approach by consideration of locally increased residual stress levels

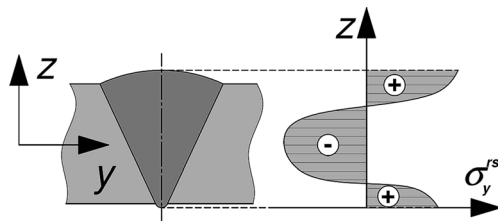


Fig. 23 Idealised schematic through thickness transverse residual stress distribution of an unrestrained butt joint

steel welds are able to plasticify during the first loading, since peak stresses reaching the yield strength, provided that the residual stress distribution across the thickness direction is self-equilibrating; see Fig. 23. Although high-strength steels show a high yield ratio, as a rule, the elevated yield strength and pronounced transformation stresses of high-strength steels lead to residual stresses that are not on the amount of the yield strength. However, overloading might lead to an earlier failure of the component as a consequence of the decreased plastic strain ratio.

Therefore, in the fracture mechanics, crack driving forces are divided in primary and secondary stresses [34]. Primary stresses arise from the applied mechanical loads (load induced stress, reaction stress), and secondary stresses are due to local residual stresses, which are self-equilibrating in the whole structure. Hence, the effect of the secondary stresses frequently depends on if the residual stresses in the section containing a crack are self-equilibrating, which is complicated to clarify.

Similar assumptions are made regarding cyclic loading of welds. It is assumed that the mean stress effect and the residual stress effect should be considered together [25]. With an increasing strength of the base and weld metal, the effects vary, since the ratio of the residual stress level to the yield strength of the material decreases. Hence, it is suggested to divide between local and global welding stresses according to their origin. Note that the discussed residual stress level in the HAZ should be taken into account, since they arise as a consequence of the global bending moment. A redistribution of stresses is then suppressed, especially in high-strength steels due to the high yield strength. Also, detrimental microstructures might lead to a premature failure of the component, particularly in combination with complex stress states. If, on the other hand, local compressive residual stress levels occur, beneficial effects considering the component performance in σ'_{21} may be contributed.

5.4 Local critical stress spots

Another consideration of σ'_{21} is due to local residual stress maxima and the assessment of residual stresses in load critical regions of the weld. This might be important in the case of the following examples.

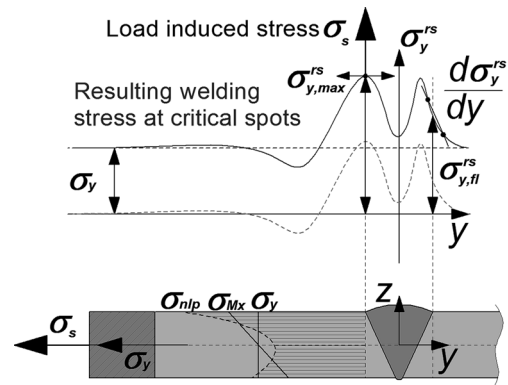


Fig. 24 Superposition of load induced stresses and stresses due to welding by consideration of local tensile residual stress maxima and material properties

For a local residual stress assessment of crane components, the transverse residual stress distributions have to be taken into account. However, an assessment of the residual stresses alone is insufficient. The consideration of the local material properties $\lambda(y)$ is necessary; see Eqs. 7.1 to 7.3. Note that high residual stress peaks in high-strength steels are usually due to near-surface effects during cooling. As a consequence, the maxima of transverse residual stresses are mainly located at the weld metal; see Fig. 24. However, the fact that crack initiation typically starts from the surface, especially if defects are present, this necessitates a high quality of the weld and its surface [25, 33]. A superposition of high residual stresses and stress intensifications due to local defects or a disadvantageous design may lead to significant earlier failures of welded components; see Eq. 7.4.

$$\sigma'_1 = \sigma'_{11} + \sigma'_{21}(\lambda(y)) \tag{7.1}$$

$$\sigma'_{11} = \sigma_s + \sigma_y \left(E, T_{p/i}, R_{Fy} \right) \tag{7.2}$$

$$\sigma'_{21} = \lambda(y) \cdot (\sigma_{Mx} + \sigma_{nlp}) \tag{7.3}$$

$$\sigma'_{rsmax} = \sigma_s + \lambda(y) \cdot \sigma_{y,max}^{rs} \tag{7.4}$$

$$\sigma'_{fl} = \sigma_s + \lambda(y) \cdot \sigma_{y,fl}^{rs} \tag{7.5}$$

Special attention should be paid to the fusion line, since fatigue behaviour in high-strength steel welds is dominated by the notch effect; see Eq. 7.5. For a utilisation of the high-strength steel potential in the face of cyclic loading, the quality of the weld becomes the dominating factor due to the high-yield ratio. As it has been shown above, the transition zone from the weld metal to the HAZ is affected by high stress gradients; see Fig. 24. Thus, the effective residual stress value in the fusion line varies significantly from case to case. Hence, a quantification and assessment is complex but recommendable. Generally, post-weld treatments are suggested to locally

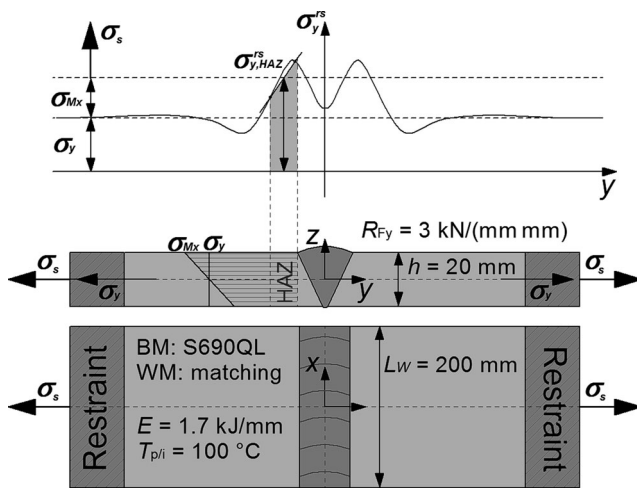


Fig. 25 Schematic for a quasi-static example calculation of the limit design stress considering local structural stresses according to the standards for mobile crane design

manipulate influences of notches and tensile residual stresses. Though, the practicability depends on the time and cost effort as well as accessibility of the weld seam.

In conservative assumptions in any load condition, the highest residual stresses are on the amount of the yield strength and are

located at the fusion line. But, also high residual stresses in the HAZ have to be judged conservatively, because of the locally reduced mechanical properties due to a detrimental microstructure. A superposition of the mean stress effect and residual stress effect leads to a parallel assessment of global welding and load-induced stresses and local residual stresses respectively. Thus, the consideration of both is necessary to supply any predictions concerning cyclic design life [25].

5.5 Example calculation

A welded member of a mobile crane is subjected to a transverse dead and hoist load; see Fig. 25. All loads are quasi-static, tensile and normal to the weld cross section. In Table 2, the maximum hoist load within the design stress is calculated comparative according to [15, 30–32] and to the introduced suggestion for local structural stresses; see Sect. 5.3. It is assumed that the most unfavourable location in the welded member is the HAZ. If the local residual stress level in the HAZ in the design stress calculation is included, a consideration of the local defects and residual stresses by a determination of the reference stress level σ_{Ed} according to the concept for the choice of steel grades for the avoidance of brittle fracture in Eurocode 3 [15] is abdicable. Besides, this reference

Table 2 Example calculation of the limit design stress according to the standards and the introduced approach for local structural stresses

Parameter	[15, 30–32]	Approach
Design stress	σ_l	σ'_l
F_1 dead load	500 kN	500 kN
F_2 hoist load	660 kN	750 kN
Dynamic factors ϕ_2 (HC2, HD5, $v_H = 0.75$ m/s)	1.23	1.23
Safety coefficients (load combination A1)		
γ_{p1} for the dead load	1.22	1.22 ^a
γ_{p2} for the hoist load	1.34	1.34 ^a
γ_n for the risk (class 1, case 3)	1.1	1.1
$\gamma_{p1}F_1$	610 kN	610 kN
$\gamma_{p2}\phi_2F_2$	1086 kN	1234 kN
Load induced stress $\sigma_S = \gamma_n(\gamma_{p1}F_1 + \gamma_{p2}\phi_2F_2)/A$ (without local effects)	466 MPa	507 MPa
Residual stress level in HAZ $\sigma_{y,HAZ}^{rs}(E, T_{p/i}, R_{Fy})$	–	120 MPa
$\sigma'_l = \sigma'_{l1} + \sigma'_{l2}$	466 MPa	627 MPa
Limit design stress	<i>lim</i> σ	<i>lim</i> σ
f_y yield strength	690 MPa	690 MPa
γ_m resistance coefficient	1.1	1.1
α_w factor for limit weld stress (normal stress, full penetration, tension)	1.0	1.0
Consideration of local defects / residual stresses by reference stress level ($T_{Ed} = -40$ °C) $\sigma_{Ed} = 0.75 \cdot f_y(t)$	513	–
$\lim\sigma = R_d/\gamma_m$	466 MPa	627 MPa

^a Checking of safety coefficients in terms of residual stress consideration; *italic: results*

stress level concept was primarily developed for lower strength steels and the maximum yield strength within this concept is 690 MPa.

Hence, following the introduced approach, the limit design stress σ for the steel grade S690QL, welded with a matching filler material, is increased. Taking into account the toughness of the member, EN 13001 provides a calculation of different toughness parameters q_i for an adequate choice of the applied steel grade in order to avoid brittle fracture.

The local and global stresses due to welding are therefore included in the design stress σ'_1 by means of the residual stress level in the HAZ $\sigma_{y,HAZ}^{rs} = \sigma'_{HAZ}$; see Eq. 6.4. It is supposed that the welding residual stress level in the HAZ includes the normal reaction stresses, Eq. 6.1, and bending stresses due to a restrained angular distortion. As a result, the maximum hoist load is 14% higher if calculated with local structural stresses approach. Note that further examinations have to be done to verify these calculations in several examples and also to check the height of the partial safety factors for the dead or hoist loads, by means of residual stress assessment.

6 Conclusions

In the present study, the interaction of the influence factors (process, design, material) on the welding stresses in high-strength steel components was investigated. Based on two recent publications [8, 12], heat control, restraint intensity and filler metal selection on local and global welding stresses were further analysed. From studies of a real crane structure, the experimental conditions were derived. Multilayer-MAG-welds were conducted in butt joints under component-related restraint in weld transverse direction. The observation of the arising local and global welding stresses with special testing facilities allowed their quantification and assessment regarding the design of load-bearing crane components. From this work, the following conclusions can be drawn:

1. Analyses of restraint conditions in real crane components provide the transferability of observed effects in laboratory experiments to realistic situations.
2. In the effect analyses of heat control, restraint intensity and applied material on the local restraint stresses, global reaction stresses and their superposition, varying results dependent on the weld region were observed. High heat input, interpass temperatures, restraint intensities and transformation start temperatures of the filler metal generally lead to higher global reaction forces.
3. The same trend was observed for the local residual stresses, due to the superposition with global reaction stresses. High restraints augment the effect of heat control parameters. In addition, the increase of the plate thickness has to

be taken into account due to the altered thermal conduction and residual stress distributions.

4. Elevated interpass temperatures associated with a high level of heat input are especially able to increase the welding stresses in critical regions of the weld under high restraint conditions. This may be detrimental in the face of overloading and premature failure considering lifetime.
5. Based on the technical guidelines for the design of crane components, an engineering approach was conducted to assess the welding stresses. The distinction of the scope of the residual stresses in a component weld allowed the consideration of the nominal and structural stresses and critical stress spots. For the latter, local material properties have to be taken into account.
6. The consideration of global welding and load-induced stresses by σ'_{11} and of the local restraint stresses and material properties $\sigma'_{21}(\lambda(\nu))$ allows a precise strength assessment by means of fitness for purpose designing high-strength steel crane components. Calculations including a superposition of those stresses and loads in critical regions might prevent too conservative assumptions as well as dangerous underestimations.

A first comparative calculation regarding crane component design showed an increased utilisation of a welded high-strength steel member using the introduced approach considering local structural stresses. In a next step, investigations regarding verification of these calculations and of the partial safety factors have to be performed at a number of typical samples.

Acknowledgements The studies were funded by the AIF-projects IGF-Nr. 17267 N/FOSTA P922 and IGF-Nr. 17978 N/FOSTA P1011. Sincere thanks are given for this support and to the representing companies actively involved in the project boards.

References

1. Hulka K, Kern A, Schriever U (2005) Application of niobium in quenched and tempered high-strength steels. *Mater Sci Forum* 500-501:519–526. doi:10.4028/www.scientific.net/MSF.500-501.519
2. Hara N, Sato M (2009) Development and application of welding consumables for 950MPa class high strength steel. *Conf, High Strength Steels Hydropower Plants*, Takasaki, Japan
3. Rauch R, Kapl S, Posch G, Radlmayr K (2012) High strength low alloy steel weldments with accommodated qualities to the base metal. *BHM Berg- und Hüttenmännische Monatshefte* 157:102–107. doi:10.1007/s00501-012-0060-5
4. Wongpanya P, Boellinghaus T, Lothongkum G (2008) Ways to reduce the cold cracking risk in high strength structural steel welds. *Int. Conf. Int. Inst. Weld.*
5. Dong P, Hong JK, Bouchard PJ (2005) Analysis of residual stresses at weld repairs. *Int J Press Vessel Pip* 82:258–269. doi:10.1016/j.ijvp.2004.08.004

6. Boellinghaus T, Kannengiesser T, Neuhaus M (2005) Effects of the structural restraint intensity on the stress strain build up in butt joints. *Math Model Weld Phenom* 7:651–669
7. Lu J (2002) Prestress engineering of structural material: a global design approach to the residual stress problem. In: *Handb. Residual Stress Deform. Steel*, pp 11–26
8. Schroepfer D, Kannengiesser T (2014) Correlating welding reaction stresses and weld process conditions for high-strength steel S960QL. *Weld World* 58:423–432. doi:10.1007/s40194-014-0127-x
9. Boellinghaus T, Kannengiesser T (2003) Effect of filler material selection and shrinkage restraint on stress strain build up in component welds. In: 6th Int. Trends Weld. Res. Conf. Proceedings, ASM International, Pine Mountain, Georgia, USA, pp 906–911
10. Rhode M, Kromm A, Kannengiesser T (2012) Residual stresses in multi-layer component welds. In: *Trends Weld. Res. Proc. 9th Int. Conf. ASM International*, ISBN: 1-62708-998-8, Chicago, Illinois, USA, pp 48–54
11. Satoh K, Ueda Y, Matsui S et al (1977) Japanese studies on structural restraint severity in relation to weld cracking. *Weld World* 15: 155–189
12. Schroepfer D, Kromm A, Kannengiesser T (2015) Improving welding stresses by filler metal and heat control selection in component-related butt joints of high-strength steel. *Weld World* 59:455–464. doi:10.1007/s40194-014-0219-7
13. Lausch T, Kannengiesser T, Schmitz-Niederau M (2013) Multi-axial load analysis of thick-walled component welds made of 13CrMoV9-10. *J Mater Process Technol* 213:1234–1240. doi:10.1016/j.jmatprotec.2013.01.008
14. Kannengiesser T, Lausch T, Kromm A (2011) Effects of heat control on the stress build-up during high-strength steel welding under defined restraint conditions. *Weld World* 55:58–65. doi:10.1007/BF03321308
15. Eurocode 3: Design of steel structures (EN 1993), 2010
16. EN 10025-6: Hot rolled products of structural steels—part 6: technical delivery conditions for flat products of high yield strength structural steels in the quenched and tempered conditions, 2011
17. EN ISO 16834: Welding consumables—wire electrodes, wires, rods and deposits for gas shielded arc welding of high strength steels—Classification, 2012
18. Karlsson L (1986) Thermal stresses in welding. In: *Therm. Stress. I*. Elsevier Science Publishers Ltd, ISBN: 0444877282, pp 299–389
19. Nitschke-Pagel T, Wohlfahrt H (2002) Residual stresses in welded joints—sources and consequences. *Mater Sci Forum* 404-407:215–226. doi:10.4028/www.scientific.net/MSF.404-407.215
20. Nitschke-Pagel T, Wohlfahrt H (1991) The generation of residual stresses due to joining processes. In: Hauk V, Hougardy H, Macherauch E (eds) *Residual stress.—Meas. Calc. Eval.* DGM Informationsgesellschaft mbH, ISBN: 3-88355-169-4, pp 121–133
21. EN ISO 14341: Welding consumables—wire electrodes and weld deposits for gas shielded metal arc welding of non alloy and fine grain steels—Classification, 2011
22. Schroepfer D, Kannengiesser T (2016) Stress build-up in HSLA steel welds due to material behaviour. *J Mater Process Technol* 227:49–58. doi:10.1016/j.jmatprotec.2015.08.003
23. Bhadeshia HKDH (1995) Possible effects of stress on steel weld microstructures. In: Cerjak H (ed) *Math. Model. weld phenomena-II*. Institute of Materials, ISBN: 978-0-901716-63-7, London, pp 71–115
24. Leggatt RH (2008) Residual stresses in welded structures. *Press Vessel Pip* 85:144–151. doi:10.1016/j.ijpvp.2007.10.004
25. Wohlfahrt H, Nitschke-Pagel T, Kaßner M (1997) *Schweißbedingte Eigenspannungen—Entstehung und Erfassung, Auswirkung und Bewertung*. In: *DVS Berichte 187*. DVS Verlag, ISBN: 978-3-87155-492-6, Düsseldorf, pp 6–13
26. Hobbacher A (2009) *Fatigue design of welded joints and components IIW-1823-07 (ex-doc. XIII-2151r4-07 / XV-1254r4-07)*. Welding Research Council, Inc
27. Niemi E, Fricke W, Maddox SJ (2006) *Fatigue analysis of welded components—designer's guide to the structural hot-spot stress approach (IIW-1430-0)*. Woodhead Publishing, ISBN: 978-1-84569-124-0
28. Fricke W (2012) *IIW recommendations for the fatigue assessment of welded structures by notch stress analysis (IIW-2006-09)*. Woodhead Publishing, ISBN: 978-0-85709-855-9
29. Hobbacher A (2004) *Recommendations for fatigue design of welded joints and components (IIW XII-1965-03/XV-1127-03)*
30. European Standard (2015) EN 13001-1 to 3: *Cranes-general design*
31. European Standard (2014) EN 13000: *Cranes-mobile cranes*
32. Federation Europeenne de la Manutention (1994) *Section V, FEM 5.004: Rules for the design of steel structures of general use mobile cranes, 2nd edn*. English
33. Sonsino CM (2009) Effect of residual stresses on the fatigue behaviour of welded joints depending on loading conditions and weld geometry. *Int J Fatigue* 31:88–101. doi:10.1016/j.ijfatigue.2008.02.015
34. Zerbst U, Ainsworth RA, Beier HT et al (2014) Review on fracture and crack propagation in weldments—a fracture mechanics perspective. *Eng Fract Mech* 132:200–276. doi:10.1016/j.engfracmech.2014.05.012